MOLECULAR AND CELLULAR BIOLOGY, Feb. 1989, p. 719–725
0270-7306/89/020719-07$02.00/0

Vol. 9, No. 2

Molecular Isolation and Analysis of the erect wing Locus in *Drosophila melanogaster*

ROBERT J. FLEMING,† SUSAN M. DESIMONE, AND KALPANA WHITE*
Department of Biology, Brandeis University, Waltham, Massachusetts 02254

Received 22 August 1988/Accepted 18 November 1988

The molecular study of the erect wing (*ewg*) locus was initiated by isolating DNA in the 1A8-1B1 interval of the X chromosome. Previous developmental genetic analyses of the mutant alleles at the *ewg* locus have demonstrated that the wild-type *ewg* product is essential during embryogenesis and is required postembryonically at least for the development of indirect flight muscle. To define the *ewg*-encoding DNA, chromosomal breakpoints that genetically flank the *ewg* locus were used. P-element-mediated transformation followed by subsequent rescue of the *ewg*-lethal alleles has defined a 11.5-kilobase genomic fragment as encoding the *ewg* locus. Northern blot analysis of transcription from this DNA has revealed a complex pattern of transcription with respect to both size and developmental profile. Tissue distribution of putative *ewg* transcription was examined by in situ hybridization to 6- to 14-h-old embryonic sections. These sections revealed that the expression of putative *ewg* messages is limited to the central nervous system-derived structures and not observed within the mesoderm during this developmental stage.

In the fruit fly, *Drosophila melanogaster*, a large array of mutations have been discovered through phenotypic wing position abnormalities or flight abnormalities (13). Several mutants with impaired flight display defects in muscle structure or organization (8, 18, 23, 26, 27). A major fraction of these mutations are expected to reside in genes that specify muscle-specific proteins. This expectation is corroborated in the cases of a few genes whose wild-type products have been characterized (1, 16, 17, 23, 26, 27). A second set of mutations may represent genes expressed in the muscle which also have expression in other tissues. Finally, a third class of mutations may identify an interesting group of genes whose expression lies outside of the mesodermal tissue but is essential to the proper development or function of muscle. The involvement of a functional nervous system in the proper development and maintenance of muscle has been recognized in vertebrate and invertebrate systems (3, 12, 14, 19, 25, 30). The recent work of Lawrence and Johnston (20) has revealed neural influence during the differentiation and development of insect musculature.

We have been studying the erect wing (*ewg*) locus in *Drosophila melanogaster* because of the interesting phenotypes associated with mutations at this locus (11; R. J. Fleming, Ph.D. thesis, Brandeis University, Waltham, Mass., 1987). Mutant flies carrying the original *ewg* mutation are flightless, display a vertical wing posture, and lack indirect flight muscles (9, 11). More severe mutations at the *ewg* locus cause embryonic lethality, indicating that the developmental requirement for the *ewg* wild-type product is not restricted to the flight musculature. Recently, a subvital hypomorphic allele, ewg^{l18}, displaying yet another phenotype has been characterized; ewg^{l18} animals are extremely hypoactive and are flight impaired, but the indirect flight muscles are present (Fleming, Ph.D. thesis). Previous genetic mosaic analysis led us to conclude that the *ewg* wild-type product is not necessary for the survival of all cell types and that the lethal focus is localized to the ventral blastoderm, the area from which the mesoderm and the nervous system are derived (11). Thus, both the phenotypic defects associated with mutant *ewg* alleles and the genetic mosaic analyses are consistent with the suggestion that the *ewg* gene product may be required in the musculature or the nervous system.

To directly address the question of tissue specificity of expression and function of the *ewg* gene, we have initiated a molecular characterization of the *ewg*-encoding DNA. The proximal to distal order for known genes in the 1A8-1B1-2 interval of the X chromosome is yellow (*y*), arthritic (*arth*), erect wing (*ewg*), and cinnamon (*cin*) (21; Fleming, Ph.D. thesis). Previously cloned DNA just distal to the gene *y* was used to begin a molecular walk towards *ewg* (2). In this paper, we report on the localization of *ewg*-encoding DNA by molecularly defining a set of chromosomal breakpoints that genetically define the left and right limits of the *ewg* gene. DNA sequences that provide the *ewg* function were delimited further by using P-element-mediated germ line transformation and subsequent rescue of ewg^{l} mutations by the transduced segment of DNA. To study tissue distribution of likely *ewg* transcripts, serial sections of staged embryos were probed with a putative antisense *ewg* RNA probe.

MATERIALS AND METHODS

Stocks. *Drosophila melanogaster* flies were raised on cornmeal-agar-molasses-yeast medium at 25°C and 60% relative humidity. A Canton-S strain was used as a source of polyadenylated (poly[A]$^+$) RNA and embryonic tissue sections. Genetic analyses of chromosomal aberrations and *ewg* mutant alleles used in this study have been reported elsewhere (11; Fleming, Ph.D. thesis). For descriptions of genetic markers see Lindsley and Grell (22).

Plasmid constructions. DNA manipulations were performed by standard techniques. *R19* was subcloned into pEMBL9. Fragments of *R19* were subcloned into pBluegene (SK$^+$ or KS$^+$; Stratagene) or into Gemini I (Promega Corp). Restriction enzymes were purchased from New England BioLabs.

DNA extraction and Southern blots. DNA was extracted from adult animals by proteinase K digestion and repeated

* Corresponding author.
† Present address: Biology Department, Yale University, New Haven, CT 06511.

phenol and phenol:chloroform extractions (28). Approximately 10 μg of genomic DNA was digested with *Eco*RI, *Bam*HI, or *Hin*dIII, fractionated on an 0.8% agarose gel, and subsequently blotted onto nitrocellulose (24). Isolated restriction fragments, phage DNA, or plasmid DNA were radiolabeled with [^{32}P]dCTP by nick translation (24). Prehybridization, hybridization, and washes were performed as described by Maniatis et al. (24). Filters were exposed to X-AR film (Eastman Kodak Co.) with a Lightning-Plus intensifying screen (Kodak) at −70°C.

RNA extraction and Northern blots. Developmentally staged material was collected from flies raised at 25°C and was rapidly frozen in liquid nitrogen. RNA was extracted by homogenization and repeated phenol and phenol:chloroform extractions. Poly(A)$^+$ RNA was isolated by passage over oligo(dT) cellulose (24). Approximately 4 μg of poly(A)$^+$ RNA from each developmental stage was fractionated on a 1% agarose gel containing 2.2 M formaldehyde and subsequently blotted onto Nytran membrane (Schleicher & Schuell, Inc.) by the instructions described by the manufacturer. Molecular weights of transcripts were determined by comparison to the 0.24-9.5-kilobase (kb) RNA ladder (Bethesda Research Laboratories). Plasmid DNA was radiolabeled with [^{32}P]dCTP by random priming (10). [^{32}P]UTP-labeled RNA was prepared by in vitro transcription with SP6, T7, or T3 RNA polymerase (7). For Northern blots probed with DNA probes, prehybridization, hybridization, filter washes, and filter stripping were performed as described by Maniatis et al. (24). However, Northern blots probed with RNA probes were hybridized in 50% formamide at 55°C and washed at 75°C to reduce background. All filters were exposed to X-AR film (Kodak) with a Lightning-Plus intensifying screen (Kodak) at −70°C.

Generation of germ line transformants. The pPA1 P-element transformation vector containing the selectable alcohol dehydrogenase (*Adh*) gene (35) was used for transformation of the *R19* fragment. The CaSpeR P-element transformation vector containing the selectable white (*w*) gene (29) was used for transformation of the proximal *Eco*RI-*Bam*HI subclone and the proximal *Pst*I-*Eco*RI subclone, and the cp20.1 P-element transformation vector containing the selectable rosy (*ry*) gene (33) was used for transformation of the internal *Hin*dIII subclone. Germ line transformants were produced by coinjection of cloned DNA (500 μg/ml) and helper plasmid pπ25.7 (50 μg/ml) (32, 34) into the appropriate recipient embryos: Adh^{fn23} *cn br* for the pPA1 construct, *Df(1)w* for the CaSpeR construct, and ry^{506} for the cp20.1 construct. G_0 adults were mated back to the same strain used for injection. Transformed F_1 progeny were selected by virtue of the selectable marker on the transformation vector.

Analysis of germ line transformants. Transformed males were mated with $ewg^{l1}y$ *cho sn*/X virgin females. The presence of phenotypically yellow, chocolate, and singed ($ewg^{l1}y$ *cho sn*/Y) adults indicated rescue of the *ewg* embryonic lethality.

In situ hybridization. The procedure used was essentially as described in Ingham et al. (15), with modifications as described in Campos et al. (4). ^{35}S-labeled RNA probes were used. Exposure time was 5 days.

RESULTS

Molecular cloning of *ewg* locus DNA. The *ewg* gene is located within the salivary segment 1A8-1B1 of the X chromosome of *Drosophila melanogaster* distal to the *y* gene (Fleming, Ph.D. thesis). To isolate *ewg*-encoding DNA, a chromosomal walk was initiated from cloned genomic DNA, which was located distal to the *y*-encoding sequences (2). The molecular map of this region as determined from the *y-ewg* walk is shown in Fig. 1. A more detailed account of this walk which extends ~80 kb distal to *y* is presented elsewhere (Fleming, Ph.D. thesis). Our data are represented by using the genomic DNA coordinates of Campuzano et al. (6), as this walk is an extension of their published walk in the 1B region. For this analysis, the ~80-kb DNA interval is divided into 21 contiguous *Eco*RI fragments, starting with the most proximal (*R1*) and ending with the most distal (*R21*), encompassing map coordinates 81 to 163.

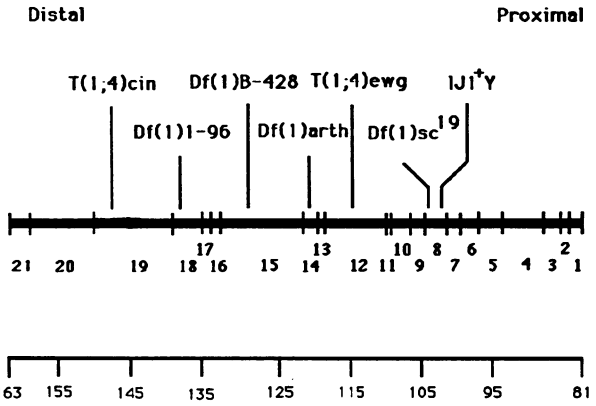

FIG. 1. Molecular map of the *y-ewg* walk. The orientation relative to the centromere is shown above the map. The region is divided into 21 contiguous *Eco*RI fragments. Only the *Eco*RI sites are depicted. The fragment numbers are indicated below the map, beginning with fragment 1 at the proximal end and extending distally to fragment 21. The genomic DNA coordinates of Campuzano et al. (6) are indicated by the scale shown below the map. The molecular breakpoints for chromosomal aberrations shown in Table 1 are indicated.

To delimit the *ewg* DNA, we took advantage of deficiency and duplication chromosomes which genetically define the proximal and distal boundaries of the *ewg* locus. The locus *ewg* is flanked by the *arth* gene proximally and the *cin* gene distally. Table 1 lists the chromosomes that are relevant to the molecular analysis presented in this paper, along with their genetic and molecular properties. The molecular locations of these chromosomal breakpoints are depicted in Fig. 1. A total of six genetic breakpoints define the *ewg* proximal

TABLE 1. Genetic and molecular properties of chromosomal breakpoints flanking *ewg*

Breakpoints	Complementation of:				*Eco*RI fragment[a]	Coordinates[b]
	cin	*ewg*	*arth*	*y*		
lJ1+Y	+[c]	+	−[d]	−	*R18*	100–103
$Df(1)sc^{19}$	+	+	−	−	*R8*	100–103
Df(1)arth	+	+	−	−	*R14*	119–121
$T(1;4)ewg^{XP4D}$	−	−	+	+	*R12*	109–118
Df(1)B-428	−	−	+	+	*R15*	121–133
Df(1)1-96	−	−	+	+	*R18*	136–140
$T(1;4)cin^{XP4D}$	−	+	+	+	*R19*	140–151

[a] *Eco*RI fragment number within the *y-ewg* molecular walk to which the breakpoint was localized. Contiguous *Eco*RI fragments were numbered consecutively, 1 to 21, starting with coordinate 81, just distal to *y*-encoding sequence and ending at coordinate 163.
[b] Coordinates of the *Eco*RI fragment.
[c] Plus sign denotes genetic complementation.
[d] Minus sign denotes noncomplementation.

border. Duplication *lJ1*$^+$*Y* covers *ewg* and distal loci but not *arth*. Two interstitial deficiencies, *Df(1) sc*^{19} and *Df(1)arth*, uncover *arth* but not *ewg*. Three terminal deletions, *T(1;4)ewg*^{XP4D}, *Df(1)B-428*, and *Df(1)1-96*, uncover *ewg* but cover *arth*. In addition, the *T(1;4)ewg*^{XD4P} segregant is known to carry the *ewg* gene (Fleming, Ph.D. thesis). A single X-terminal deficiency breakpoint, *T(1;4)cin*^{XP4D}, defines the distal border of the *ewg* locus as it retains the *ewg* function but not the *cin* function.

Molecular breakpoints of the seven duplication or deficiency chromosomes were localized to *Eco*RI fragments by genomic Southern blot analyses of DNA isolated from flies carrying the chromosome of interest (Table 1; Fig. 1). The most distal molecular breakpoint of the three chromosomal deficiencies between *ewg* and *arth* [*lJ1*$^+$*Y*, *Df(1)sc*^{19}, and *Df(1)arth*] which retain the *ewg* function is that of *Df(1)arth* within the fragment *R14* (coordinates 119 to 121). The molecular breakpoints of the terminal deletion chromosomes *Df(1)B-428* (in *R15*) and *Df(1)1-96* (in *R18*) are distal to the *Df(1)arth* breakpoint; however, since the terminal deletions fail to complement mutant *ewg* alleles, they may be either completely deficient for the gene or break within the gene. These data place the proximal border of *ewg* in the *R14* fragment (coordinates 119 to 121). Finally, the *T(1;4)cin*^{XP4D} breakpoint, defining the distal *ewg* border, was localized to fragment *R19* (coordinates 140 to 151) and within the *R19* fragment to a *Bam*HI-*Hin*dIII fragment (coordinates 147 to 149). The molecular localization of these breakpoints limits the *ewg*-encoding region to a maximum of about 30 kb of DNA (coordinates 119 to 149).

DNA extracted from the mutant alleles *ewg*, *ewg*^{l1} through *ewg*^{l7}, and *ewg*^{l18} was examined on genomic Southern blots with probes spanning the delimited *ewg* region (coordinates 119 to 149). Restriction fragment alterations that correlate with the mutant phenotypes were not observed for any of these alleles.

Localization of *ewg* to the *R19 Eco*RI fragment by germ line transformation. The *ewg* DNA, as determined by the genomic breakpoint analyses, lies between positions 119 and 149. To delimit the gene further, transcriptional activity of the putative *ewg* DNA (*R15* through *R19*) was determined. We reasoned that *ewg*-encoding DNA must be transcribed during embryogenesis, as the *ewg* mutant alleles cause embryonic lethality. Northern (RNA) blots of poly(A)$^+$ RNA extracted from 9- to 24-h-old embryos were probed with subclones *R15*, *R16*, *R18*, and *R19*. The *R15* subclone detects a single poly(A)$^+$ RNA transcript which is ~5.0 kb in size, and *R16* and *R18* probes do not detect embryonic transcripts (data not shown). The *R19* subclone (Fig. 2) detects numerous transcripts ranging from 0.7 to 6.0 kb (Fig. 3A and B).

To ascertain if either of these transcriptionally active regions (*R15* or *R19*) is sufficient for proper *ewg* function, P-element-mediated germ line transformation experiments were conducted with the *R15* and *R19* genomic fragments. Three independent transformed lines were recovered for each fragment. Each line was tested for the ability of the transduced insert to rescue the lethal phenotype of the *ewg*^{l1} mutation. Only the lines transformed with the *R19* fragment were capable of restoring *ewg* function. The two autosomal inserts, *Tf(3)ewgR19*^{1} and *Tf(3)ewgR19*^{3}, as well as the X-linked insert *Tf(1)ewgR19*^{2}, are able to rescue the lethality caused by mutant alleles of *ewg* (Table 2). Rescue by the autosomal inserts is near 100% for all alleles tested. The X-linked insert *Tf(1)ewgR19*^{2} does not rescue *ewg*-lethal alleles as effectively as the autosomal inserts. To date, the reason for incomplete rescue by *Tf(1)ewgR19*^{2} is unclear.

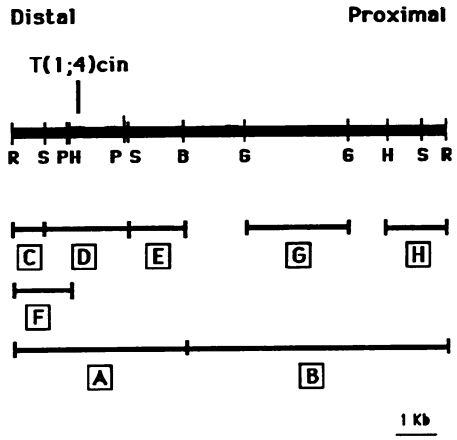

FIG. 2. Molecular map of the *ewg*-encoding *R19* fragment. The orientation, relative to the centromere, is shown above the map. Only the restriction sites used to generate subclones discussed in this work are shown. R (*Eco*RI), S (*Sac*I), P (*Pst*I), H (*Hin*dIII), G (*Bgl*II), and B (*Bam*HI). The molecular breakpoint for *T(1;4)cin*^{XP4D} is also shown. Sequences distal to the breakpoint are deleted from the translocation chromosome. Each of the designated subclones, boxed letters A to H, was used to probe developmental RNA blots containing staged poly(A)$^+$ RNA from embryos, pupae, and adult flies. Subclone G was also used as a probe for in situ hybridization to 6- to 12-h-old embryos. Subclones C, E, and H did not detect any messages. Subclones A and B each recognize a different group of transcripts, designated the distal or proximal family, respectively.

Rescue of *ewg*-lethal alleles by the transduced *R19* fragment indicates that most or all of the essential *ewg* DNA sequences lie within it (Fig. 2). It is interesting to note that the *T(1;4)cin*^{XP4D} breakpoint is localized within fragment *R19*, immediately proximal to the distal *Hin*dIII site (Fig. 2). In situ hybridization of the distal *Hin*dIII-*Eco*RI to the salivary chromosome squashes of the *T(1;4)cin*^{XP4D} chromosome confirms that these sequences are absent from the translocated chromosome (data not shown). Since *T(1;4)cin*^{XP4D} deletes the distal *Hin*dIII-*Eco*RI fragment but still retains *ewg* function, essential *ewg* sequences must lie within the proximal ~9.5-kb DNA represented by the *Eco*RI-*Hin*dIII fragment (Fig. 2).

To further delimit the *ewg* locus within the 11.5-kb *R19* fragment, germ line transformants were created with the proximal *Eco*RI-*Bam*HI fragment (Fig. 2, subclone B) and the internal *Hin*dIII genomic fragment (Fig. 2). Two independent transformed lines with autosomal inserts were recovered with the B subclone, and one line was recovered for the internal *Hin*dIII fragment. Each line was tested for the ability to rescue the lethal phenotype caused by the *ewg*^{l1} mutation. Both inserts were unable to rescue the lethality caused by the *ewg*^{l1} mutation, indicating that sequences outside the proximal *Hin*dIII-*Bam*HI fragment are important for the *ewg* vital function. The alternative possibility, that the inability of these inserts to rescue the lethality of the *ewg*^{l1} allele is a consequence of position effect, is unlikely, based on results described below.

To determine if sequences distal to the *Bam*HI site are necessary for *ewg* vital function, germ line transformants were constructed with the proximal *Eco*RI-*Pst*I fragment (Fig. 2). In preliminary analysis, four independent transformed lines were able to rescue the lethal phenotype caused by the *ewg*^{l1} mutation. These results indicate that the essen-

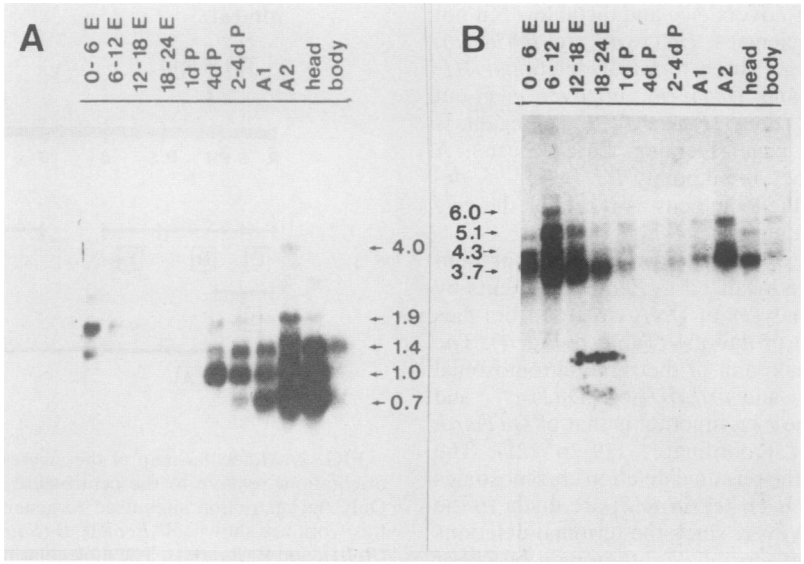

FIG. 3. Developmental pattern of transcription from the *ewg*-encoding genomic fragment *R19*. Poly(A)$^+$ RNA from embryos (E) aged 0 to 6, 6 to 12, 12 to 18, and 18 to 24 h, pupae (P) aged 1, 2 to 4, and 4 days, adults (A), adult heads, and adult bodies was electrophoresed on a 1% agarose–2.2 M formaldehyde gel and processed for RNA blotting, hybridization, and stripping as described in Materials and Methods. Each lane contains approximately 4 μg of poly(A)$^+$ RNA (except that lane A2 contains 26 μg). (A) The blot was probed with the distal *Eco*RI-*Bam*HI fragment of *R19* (subclone A in Fig. 2). (B) The blot used in 3A was stripped and reprobed with the proximal *Eco*RI-*Bam*HI fragment of *R19* (subclone B in Fig. 2). Appropriate molecular size markers were not present on this blot. The approximate molecular sizes (in kb) of transcripts as determined from other blots are indicated beside the autoradiograms.

tial *ewg* sequences are contained in the proximal *Eco*RI-*Pst*I fragment.

Transcription of *ewg*-encoding DNA. Transcription from the genomic 11.5-kb *R19* fragment was analyzed by probing RNA blots of developmentally staged poly(A)$^+$ RNA with the entire fragment. Numerous developmentally regulated transcripts were detected. To better define the transcription from this region, subcloned fragments of *R19* depicted in Fig. 2 were used as probes for RNA blots. Figure 3 shows the results of probing developmental RNA blots prepared from poly(A)$^+$ RNA from embryonic, pupal, and adult stages with the distal *Bam*HI-*Eco*RI subclone and the proximal *Eco*RI-*Bam*HI subclone (Fig. 2, subclones A and B). This approach revealed that the *R19* fragment contains two apparently distinct families of transcripts. One set, referred to as the proximal family, arises from sequences within the *Eco*RI-*Sac*I region (Fig. 2, subclones B and E), whereas the other set, referred to as the distal family, is transcribed from sequences distal to the internal *Bam*HI site (Fig. 2, subclone A). Neither family of transcripts is detected by the *R18* and *R20* fragments (data not shown). The proximal family is likely to contain *ewg* transcripts, as transformant flies bearing only the proximal *Eco*RI-*Pst*I fragment are able to restore *ewg* function and the DNA represented by the distal subclone C is deleted in the $T(1;4)cin^{XP4D}$ chromosome.

The exact number of individual transcripts detected by the proximal region was difficult to determine because the bands in the autoradiograms were somewhat diffused. However, bands on the same RNA blot revealed by the probes for the distal family were distinct (Fig. 3A and B). Our best estimate is that the proximal family consists of at least five transcripts that range in size from 3.7 to 6.0 kb. From RNA blots probed with individual subclones E, G, H, and B, we conclude that the transcriptionally active genomic region is within the 5.1-kb *Hin*dIII-*Bam*HI fragment, whereas DNA represented by subclones E and H appears to be transcriptionally silent. However, since the larger transcripts are in the 6.0-kb range, at least a part of E or H or both must also be transcribed. Transcription of the proximal family is most pronounced in 6- to 12-h-old embryos and decreases during the second half of embryogenesis. A subset of the transcripts seen in 6- to 12-h-old embryonic RNA, probably 3, is present in 0- to

TABLE 2. Viability index of $ewg^{l\#}/ewg^{l1}$ mutant flies carrying transduced *R19* DNA[a]

Breakpoints[b]	ewg^{l1}	ewg^{l2}	ewg^{l3}	ewg^{l4}	ewg^{l5}	ewg^{l6}
*Tf(3)*ewg*R19*^{1}	0.98 (114/232)	1.11 (64/115)	0.85 (85/199)	0.74 (21/57)	1.36 (142/208)	0.78 (74/189)
Tf(3)ewgR19^3	0.92 (78/168)	0.88 (112/256)	0.84 (72/171)	0.78 (65/166)	0.89 (95/213)	1.18 (67/114)
Tf(1)ewgR19^2	0.14 (38/273)	0.45 (133/295)	0.17 (69/407)	0.19 (54/289)	0.14 (60/439)	0.42 (131/309)

[a] For autosomal inserts, males of the genotype ewg^{l1}/Y; *Tf(3)ewgR19*$^{\#}$*/TM3 Sb* were crossed to females of a given mutant allele ($ewg^{l\#}$/X-balancer). Among the progeny of this cross, all mutant females ($ewg^{l\#}/ewg^{l1}$) are expected to die unless the *R19* fragment provides *ewg* function. Since only half of the females will carry the insert, the viability index was defined as 2(number of mutant *ewg* gene-carrying females)/number of X-balancer-carrying females. A viability index of 1 indicates complete rescue of the lethal allele; a viability index greater than 1 is due to partial dominant lethality associated with the balancer chromosome. For the X-linked insert, the insert was first crossed into a ewg^{l1}-bearing chromosome. Complementation tests were done by crossing ewg^{l1} *y cho Tf(1)ewgR19*^{2}*/Y* males to females of genotype $ewg^{l\#}$/X-balancer. The survival index was calculated as the number of mutant *ewg* gene-carrying females (ewg^{l1} *y cho Tf(1)ewgR19*^{2}/$ewg^{l\#}$)/number of X-balancer-carrying females (ewg^{l1} *y cho Tf(1)ewgR19*^{2}/X-balancer).

[b] *Tf* stands for the transformant; the numbers in parentheses indicate the chromosomal linkage; *ewgR19* stands for the *R19 Eco*RI fragment used. Superscripts 1 to 3 represent separate lines.

6-h-old embryonic RNA. A different but overlapping subset, probably 4, is present in the adults (Fig. 3B). One of the adult transcripts, ~5.2 kb in size, appears to be head specific (Fig. 3B), as it is detected only in the RNA samples prepared from the fly heads but not detected in samples prepared from the fly bodies. The direction of transcription for the proximal family of embryonic transcripts is judged to be proximal to distal as determined by hybridization with single-stranded RNA probes (data not shown).

There are at least five transcripts in the distal family of transcripts, ranging in size from 0.7 to 4.0 kb (Fig. 2A). These transcripts are highly expressed in adult heads. A small subset of this family can be detected in the poly(A)$^+$ RNA prepared from 0- to 6- and 6- to 12-h-old embryos.

Tissue specificity of *ewg* expression. To determine if the embryonic requirement of *ewg* is tissue specific and, in particular, if it is mesodermal or neural or both, the tissue distribution of putative *ewg* transcripts was analyzed. RNA blot analysis has shown that, during embryogenesis, the most abundant expression of all the putative *ewg* transcripts occurs in the 6- to 12-h-old embryos. Tissue sections prepared from 6- to 14-h-old embryos were hybridized to ^{35}S-labeled RNA transcribed from the 3.0-kb *Bgl*II fragment (Fig. 2, subclone G). The entire proximal family of transcripts is detected by this probe. Only the proximal family of transcripts was analyzed by in situ hybridization, as the transformation data and the analysis of the *T(1;4)cin^{XP4D}* chromosome both indicate that this family contains the likely *ewg* transcripts.

Figure 4 depicts an autoradiogram of an approximately 10- to 11-h-old embryo (at 25°C) following hybridization with the subclone G antisense strand. Transcription is evident in the developing brain and the ventral nervous system, but not in the mesodermal derivatives. This pattern of expression was observed in all embryos examined (61/61). Hybridization with the sense strand does not reveal localized grains (data not shown). Developing somatic musculature can be seen in embryos from slightly later stages. As before, silver grains are only detected over the nervous system and not over the mesodermally derived structures (Fig. 5, A, B, and C).

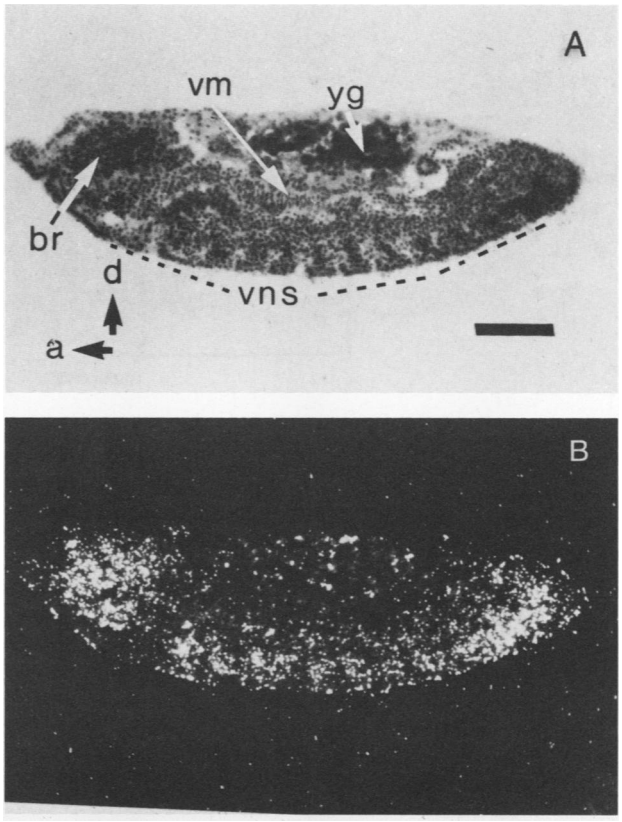

FIG. 4. Distribution of *ewg* transcripts in embryos. Representative tissue section of a stage 13-14 embryo hybridized with antisense RNA probe (subclone G in Fig. 2). Photomicrographs show a sagittal section: A, bright field; B, dark field. Abbreviations: br, brain lobe; vm, visceral mesoderm; vns, ventral nervous system; yg, yolk granules; a, anterior; d, dorsal. Bar, 50 μm. Note grains over the brain and ventral nervous system and absence of grains over the visceral mesoderm.

DISCUSSION

Molecular localization of genetically defined chromosomal breakpoints limited DNA encoding *ewg* to a ~30-kb region. With a combination of transcriptional analysis and P-element-mediated germ line transformation, the essential *ewg* region was limited further to 11.5 kb of DNA (*R19* fragment). Location of the *T(1;4)cin^{XP4D}* breakpoint further reduced the essential *ewg* sequences to the proximal 9.5 kb of the transduced 11.5-kb *R19* fragment. The terminal deficiency breakpoints, *Df(1)B-428* and *Df(1)1-96*, which genetically could have been proximal to, or within, the *ewg* sequences, have been shown to lie proximal to the *ewg* gene.

Transcription from within the *R19* fragment is limited to the central 9.5 kb proximal to the distal *Hin*dIII site (Fig. 2). The complex pattern of transcription can be subdivided into two families of transcripts, a proximal set and a distal set. Given that transformation with the proximal *Eco*RI-*Pst*I fragment restores *ewg* function and that the *T(1;4)cin^{XP4D}* chromosome deletes sequences within the distal family, the proximal family of transcripts is the best candidate for the *ewg* transcriptional unit.

The in situ hybridization data demonstrates that the initial embryonic *ewg* transcription is localized exclusively to the nervous system. Silver grain distributions over the cortical areas of the nervous system appear to be uniform (Fig. 4 and 5). Subclone G (Fig. 2), from which the antisense strand was synthesized, hybridizes to all five transcripts. Thus, the autoradiographs represent localization of all the transcripts.

Detailed understanding of the spatial distribution of *ewg* transcripts within different neural cell types, tissue distribution during later developmental stages, and distribution of individual transcripts will require further study. The *ewg*-associated transcripts in the nervous system are observed at a time when cellular proliferation and neuronal differentiation are occurring (5). We previously have observed a neural-specific embryonic transcript distribution for the embryonic-lethal abnormal visual system (*elav*) gene in *Drosophila* (4). In the case of *elav*, the neural specificity of expression appears to be retained during postembryonic and adult stages (31).

Neural-specific transcription of the *ewg* locus in the embryo at a time of its highest level of expression rules out the possibility of *ewg* being a muscle-specific gene. This finding is unexpected in light of the known defects in the indirect flight muscles in adult animals with the *ewg* gene. However, the muscle defect caused by some *ewg* alleles is only one phenotype associated with mutations at this locus. Other phenotypes include hypoactivity (Fleming, Ph.D. thesis) and embryonic lethality (11). The existence of such phenotypes,

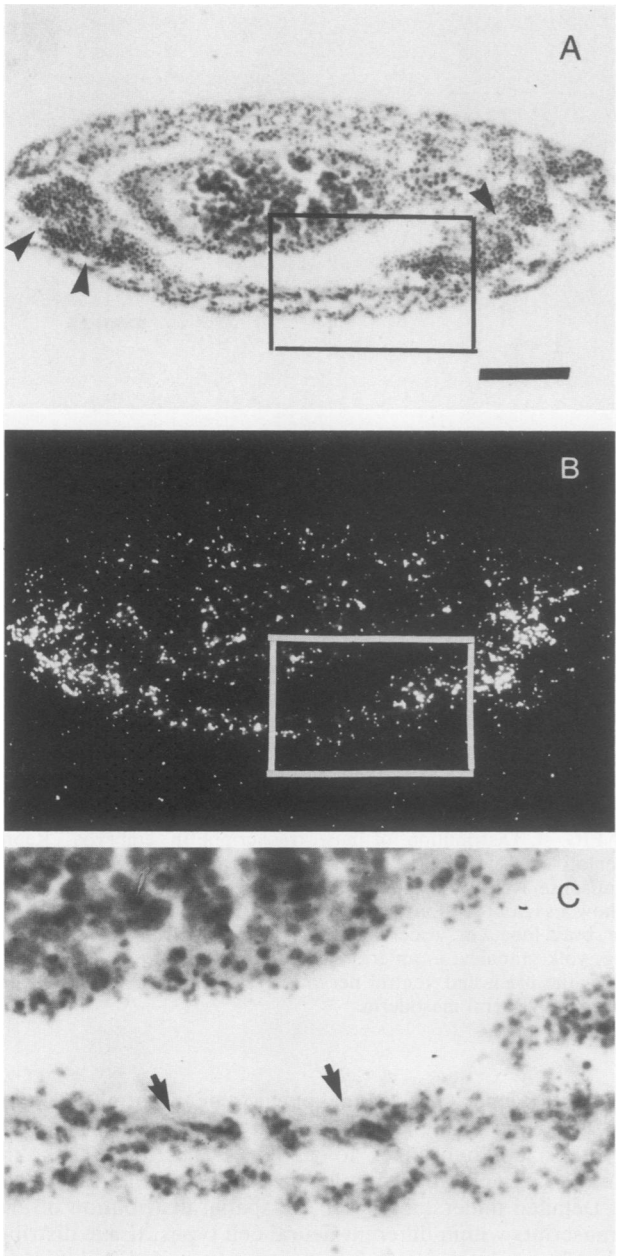

FIG. 5. *ewg* is not transcribed in the developing musculature. Representative tissue section of approximately a stage 15 embryo hybridized with antisense RNA probe (subclone G in Fig. 2). Photomicrographs: A, bright field; B, dark field; C, bright field view of the boxed area in A and B at a higher magnification showing the muscle fibers. Arrowheads in A point to the neural tissue, and arrows in C point to the muscle fibers. Note that the grains are localized to the neural tissue and not over the muscle fibers. Bar, 50 μm.

as well as the lethal focus mapping data (11), are consistent with neural expression of *ewg*.

Our data suggest that the embryonic-lethal phenotype associated with severe *ewg* mutations results from dysfunction in the nervous system. The possibility that *ewg* may be expressed in the nervous system of the embryo and subsequently expressed in other tissue types, particularly indirect flight muscles, cannot be ruled out at this time. Whether or not the indirect flight muscle defect associated with aberrant *ewg* expression is related directly to neural expression must await investigation of *ewg* expression at later developmental stages.

In the event that *ewg* expression remains neural specific throughout development, the possibility that *ewg* may be representative of a class of genes involved in the inductive effects of neural tissue on muscle formation as noted in numerous systems (12, 20, 25, 30) will have to be considered.

ACKNOWLEDGMENTS

We are indebted to H. Biessmann for providing us the subclones from the yellow region. We thank Welcome Bender, Dan Curtis, Qiang Yu, and Ana Campos for genomic libraries, and Ana Campos and Linda Martin-Morris for poly(A)$^+$ RNAs. Genetic complementation data was provided by Daniel Levin. We are grateful to Steven Robinow for help with in situ technique and Tim Tully for critical reading of the manuscript. Parts of this work were submitted by R.J.F. in partial fulfillment of the requirements for the degree of Doctor of Philosophy at Brandeis University.

The work was supported by Public Health Service grant GM-33205 from the National Institutes of Health. R.J.F. and S.M.D. were supported by predoctoral training grant GM-07122 from the National Institutes of Health.

LITERATURE CITED

1. **Bernstein, S. I., K. Mogami, J. J. Donady, and C. P. Emerson.** 1983. *Drosophila* muscle myosin heavy chain encoded by a single gene in a cluster of muscle mutations. Nature (London) **302**:393–397.
2. **Biessmann, H.** 1985. Molecular analysis of the yellow gene region of *Drosophila melanogaster*. Proc. Natl. Acad. Sci. USA **82**:7369–7373.
3. **Bonner, P. H., and T. R. Adams.** 1982. Neural induction of chick myoblast differentiation in culture. Dev. Biol. **90**:175–184.
4. **Campos, A. R., D. R. Rosen, S. N. Robinow, and K. White.** 1987. Molecular analysis of the locus *elav* in Drosophila melanogaster: a gene whose expression is neural specific. EMBO J. **6**:425–431.
5. **Campos-Ortega, J. A., and V. Hertenstein.** 1985. The embryonic development of *Drosophila melanogaster*. Springer-Verlag, New York.
6. **Campuzano, S., L. Carramolino, C. B. Cabrera, M. Ruiz-Gomez, R. Willares, A. Boronat, and J. Modelell.** 1985. Molecular genetics of the achaete-scute gene complex of *D. melanogaster*. Cell **40**:327–338.
7. **Davis, L. G., M. D. Dibner, and J. F. Battey.** 1987. Basic methods in molecular biology. Elsevier Science Publishing, Inc., New York.
8. **Deak, I. I.** 1977. Mutations of *Drosophila melanogaster* that affect flight muscles. J. Embryol. Exp. Morphol. **40**:35–63.
9. **Deak, I. I.** 1978. Thoracic duplications in the mutant wingless of *Drosophila* and their effect on muscles and nerves. Dev. Biol. **66**:422–441.
10. **Feinberg, A. P., and B. Vogelstein.** 1983. A technique for radiolabeling DNA restriction endonuclease fragments to high specific activity. Anal. Biochem. **132**:6–13.
11. **Fleming, R. J., S. Zusman, and K. White.** 1983. Developmental genetic analysis of lethal alleles at the *ewg* locus and their effects on muscle development in *Drosophila melanogaster*. Dev. Genet. **3**:347–363.
12. **Govind, C. K., and K. S. Kent.** 1982. Transformation of fast fibres to slow prevented by lack of activity in developing lobster muscle. Nature (London) **298**:755–757.
13. **Hall, J. C.** 1982. Genetics of the nervous system. *Drosophila*. Q. Rev. Biophys. **15**:223–479.
14. **Harris, A. J.** 1981. Embryonic growth and innervation of rat skeletal muscles. I. Neural regulation of muscle fibre numbers. Philos. Trans. R. Soc. Lond. B Biol. Sci. **193**:257–277.
15. **Ingham, P. W., K. R. Howard, and D. Ish-Horowitcz.** 1985. Transcription pattern of the *Drosophila* segmentation gene

hairy. Nature (London) **283**:310–312.
16. **Karlik, C. C., M. D. Coutu, and E. A. Fyrberg.** 1984. A nonsense mutation within the Act88F actin gene disrupts myofibril formation in *Drosophila* indirect flight muscles. Cell **38**: 711–719.
17. **Karlik, C. C., and E. A. Fyrberg.** 1985. An insertion within a variably spliced *Drosophila* tropomyosin gene blocks accumulation of only one encoded isoform. Cell **41**:57–66.
18. **Koana, T., and Y. Hotta.** 1978. Isolation and characterization of flightless mutants in *Drosophila melanogaster*. J. Embryol. Exp. Morphol. **45**:123–143.
19. **Kopec, S.** 1923. The influence of the nervous system on the development and regeneration of muscles and integument in insects. J. Exp. Zool. **37**:15–25.
20. **Lawrence, P. A., and P. Johnston.** 1986. The muscle pattern of a segment of *Drosophila* may be determined by neurons and not by contributing myoblasts. Cell **45**:505–513.
21. **Lefevre, G.** 1981. The distribution of randomly recovered X-ray induced sex-linked genetic effects in *Drosophila melanogaster*. Genetics **99**:461–480.
22. **Lindsley, D. L., and E. H. Grell.** 1968. Genetic variations of *Drosophila melanogaster*. Carnegie Inst. Wash. Publ. 627.
23. **Mahaffey, J. W., M. D. Coutu, E. A. Fyrberg, and W. Inwood.** 1985. The flightless *Drosophila* mutant raised has two distinct genetic lesions affecting accumulation of myofibrillar proteins in flight muscles. Cell **40**:101–110.
24. **Maniatis, T., E. F. Fritsch, and J. Sambrook.** 1982. Molecular cloning: a laboratory manual. Cold Spring Harbor Laboratory, Cold Spring Harbor, New York.
25. **Mclennan, I. S.** 1983. Neural dependence and independence of myotube production in chicken hindlimb muscles. Dev. Biol. **98**:287–294.
26. **Mogami, K., and Y. Hotta.** 1981. Isolation of *Drosophila* flightless mutants which affect myofibrillar proteins in indirect flight muscle. Mol. Gen. Genet. **183**:409–417.
27. **Mogami, K., Y. Nonomura, and Y. Hotta.** 1981. Electron microscopic and electrophoretic studies of a *Drosophila* muscle mutant wings-up B. Jpn. J. Genet. **56**:51–56.
28. **Pirrota, V., C. Hadfield, and G. H. J. Pretorius.** 1983. Microdissection and cloning of the white locus and the 3B1-3C2 region of the *Drosophila* X chromosome. EMBO J. **2**:927–934.
29. **Pirrotta, V., H. Stellar, and M. P. Bozzetti.** 1985. Multiple upstream regulatory elements control the expression of the *Drosophila* white gene. EMBO J. **4**:3501–3508.
30. **Powell, J. A., B. Friedman, and A. Cossi.** 1979. Tissue culture study of murine muscular dysgenesis: role of spontaneous action potential generation in the regulation of muscle maturation. Annu. Rev. N.Y. Acad. Sci. **317**:550–570.
31. **Robinow, S., and K. White.** 1988. The locus *elav* of *Drosophila* is expressed in neurons of all developmental stages. Dev. Biol. **126**:294–303.
32. **Rubin, G. M., and A. C. Spradling.** 1982. Genetic transformation of Drosophila with transposable element vectors. Science **218**:348–354.
33. **Simon, J. A., C. A. Sutton, R. B. Lobell, R. L. Glaser, and J. T. Lis.** 1985. Determinants of heat shock-induced chromosome puffing. Cell **40**:805–817.
34. **Spradling, A. C., and G. M. Rubin.** 1982. Transposition of cloned P-elements into *Drosophila* germ-line chromosomes. Science **218**:341–347.
35. **Zehring, W. A., D. A. Wheeler, P. Reddy, R. J. Konopka, C. P. Kyriacou, M. Rosbash, and J. C. Hall.** 1984. P-element transformation with period locus DNA restores rhythmicity to mutant, arrhythmic *Drosophila melanogaster*. Cell **39**:369–376.